

Synthesis and Characterization of Novel Ethylene-*graft*-Ethylene/Propylene Copolymers

Florian J. Stadler,^{*,†,§} Burçak Arikon-Conley,^{‡,⊥} Joachim Kaschta,[†] Walter Kaminsky,[‡] and Helmut Münstedt[†]

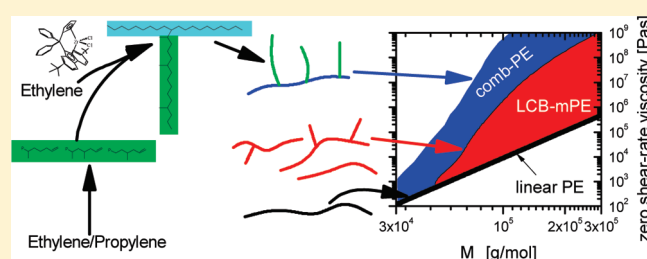
[†]Institute of Polymer Materials, Department of Materials Science, University Erlangen-Nürnberg, Martensstr. 7, D-91058 Erlangen, Germany

[‡]Institute of Technical and Macromolecular Chemistry, University Hamburg, Bundesstr. 45, D-20146 Hamburg, Germany

[§]School of Semiconductor and Chemical Engineering, Chonbuk National University, Baekjero 567, Deokjin-gu, Jeonju, Jeonbuk 561-756, Republic of Korea

 Supporting Information

ABSTRACT: A sequential metallocene-catalyzed synthesis of ethylene/propylene macromers, which are subsequently incorporated into growing polyethylene chains, leads to comb-like polymers. After the synthesis, a Soxhlet extraction ensures the purity of the sample. The GPC-MALLS analysis reveals narrowly distributed samples with a non-negligible degree of branching. The comb polymers show a very high viscosity, which significantly differs from conventional long-chain branched metallocene polyethylenes (LCB-mPE) but is in agreement with findings on comb model polymers. The zero shear rate viscosity η_0 lies significantly above the relation between M_w and η_0 for linear and for conventional LCB-mPE. The thermorheological behavior is complex and differs from that observed for LCB-mPE but also does not resemble an LDPE-like thermorheological behavior.



INTRODUCTION

Polyethylenes produced by metallocene/MAO systems have gained more and more commercial importance because of their superior material properties. However, the lack of a pronounced shear thinning and strain hardening is a significant problem for industrial applications. One strategy to adjust the properties of this class of materials is the generation of long-chain branches (LCB). The introduction of LCB with metallocene catalysts is achieved by a copolymerization of ethylene and chains terminated by a vinyl end group.¹ An enhancement of the LCB content has been tried by adding long vinyl-terminated chains, so-called macromers, to the reactor, thus increasing the availability of potential LCB.^{2,3} Until recently, only ethylene-based macromers were used,^{2,3} since they consist of sterically unhindered vinyl end groups which are able to be inserted easily, thus forming LCB. Long-chain branched polymers were produced with this method by copolymerization of ethylene-based macromers with ethylene or propylene monomers.^{2,3} However, the separation of nonincorporated ethylene-based macromers from the long-chain branched product is not easy and in most cases yields insufficient material quantities after the separation process. An improvement can be achieved by the synthesis of ethylene/propylene macromers, which exhibit low crystallinity.⁴ With this approach, it is not only possible to separate highly crystalline long-chain branched polyolefins from excess macromers (of a low crystallinity) but also to create polyolefins with novel properties, which can be very interesting for various industrial applications.

Although such ethylene/propylene amorphous or partially crystalline macromers are well-known, the main problem is to create materials consisting of sterically unhindered vinyl end groups which are, thus, able to act as macromers (this means that no side group may be at the β - and γ -position of the macromer).

It was established before⁴ that the following approach is suitable for the synthesis of macromers and, thus, comb-PE, the arms of which are incorporated macromers (Figure 1). The synthesis includes two steps. As a first step, ethylene/propylene macromers are synthesized by using the catalyst $(\text{CpMe}_5)_2\text{ZrCl}_2$, which has the special property to terminate growing chains with a 1,3-insertion of propylene; i.e., the catalyst incorporates a propene in a way that no methyl side group is produced and then terminates the reaction, leaving a high percentage of vinyl groups without a methyl group at the α - or β -position. Such moieties are sterically hindered and, thus, the biggest hindrance to produce long-chain branched polypropylene by metallocene catalysts without any special agents, such as vinyl chloride⁵ or α - ω -dienes.⁶ This macromer is subsequently fed into a reactor using ethene and the catalyst system $[\text{Ph}_2\text{C}(2,7\text{-di-}t\text{-Bu}_2\text{Flu})(\text{Cp})]\text{ZrCl}_2/\text{MAO}$ to copolymerize the macromer with the ethylene to produce long-chain branched macromer polyethylene.

Received: March 15, 2011

Revised: April 15, 2011

Published: May 20, 2011

A) Preparation of ethylene/propylene macromers

B) Copolymerization of ethylene with ethylene/propylene macromers:

Control of molar mass with H₂

Separation of excess macromers by

Soxhlet extraction

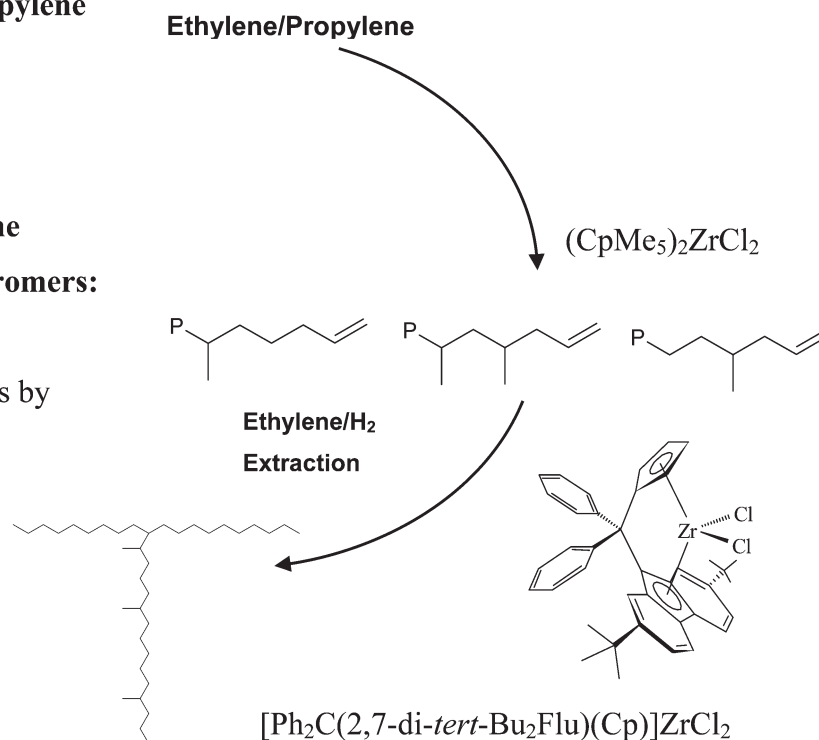


Figure 1. Reaction scheme for ethylene-graft-ethylene/propylene copolymers (P stands for the polymer main chain).

Table 1. Molecular Properties and Zero Shear Rate Viscosity η_0^a

| | run | c_{ethylene} [mol/L] | MM % in the feed | n_c [mol %] | w_c [wt %] | T_m [°C] | M_w [g/mol] | M_w/M_n | η_0 at 150 °C [Pa·s] |
|---------|-----|-------------------------------|------------------|---------------|--------------|------------|---------------|-----------|---------------------------|
| MM-0h | 2 | | 0 | 0 | 0 | 136 | 101 000 | 2 | 3.0×10^4 |
| MM-0.5h | 3 | | 0.5 | 0.16 | 31.4 | 134 | 105 000 | 1.8 | $>2.8 \times 10^6$ |
| MM-1h | 4 | 0.1 | 1 | 0.17 | 32.7 | 132 | 120 000 | 1.8 | $\gg 1.4 \times 10^8$ |
| MM-2h | 5 | | 2 | 0.31 | 47.1 | 130 | 78 000 | 2.1 | 3.5×10^5 |
| MM-5h | 6 | | 5 | 0.58 | 60.4 | 126 | 122 000 | 2.7 | $\gg 1.3 \times 10^7$ |
| MM-0l | 7 | | 0 | 0 | 0 | 136 | 33 000 | 2.0 | 142 |
| MM-0.5l | 8 | | 0.5 | 0.20 | 36.4 | 134 | 30 500 | 1.7 | n.d. |
| MM-1l | 9 | 0.05 | 1 | 0.26 | 42.7 | 131 | 32 700 | 1.7 | n.d. |
| MM-2l | 10 | | 2 | 0.35 | 50.4 | 129 | 34 000 | 2.0 | 538 |
| MM-5l | 11 | | 5 | 0.515 | 59.7 | 121 | 39 000 | 2.1 | 280 |

^a n_c = molar (macro-)comonomer content; w_c = weight (macro-)comonomer content.

In order to prove the incorporation of macromers, three methods are available. As the macromers contain methyl side groups, but the main chain does not, even the concentration of the macromers can be detected by NMR (nuclear magnetic resonance spectroscopy). It follows from the amount of methyl groups in the branched material compared to that in the macromer.³ The second method is to measure the coil contraction by GPC-MALLS, which is caused by the macromers being included within the coil of the main chain.

A very sensitive method for the detection of long-chain branches is rheological properties.^{7,8}

While the linear viscoelastic behavior of monodisperse combs is relatively well understood, the knowledge on the nonlinear behavior is still very limited, as only very few reports exist on elongational viscosity,⁹ large-amplitude oscillatory shear,^{10,11} and relaxation behavior and damping functions.¹²

For the characterization of long-chain branches in polyolefins in the linear viscoelastic regime several different methods have been reported. Linear polymers follow the well-known correlation between the zero shear rate viscosity η_0 and the weight-average molar mass M_w with an exponent of around 3.4,^{13,14} which was recently shown to be valid for HDPE and LLDPE of a very wide range of molar masses, molar mass distributions, and comonomer contents.^{15–17} The introduction of some few long-chain branches, in general, leads to a failure of that correlation toward higher zero shear-rate viscosities η_0 .^{8,18–21}

The introduction of long-chain branches also results in an increase of the steady-state recoverable compliance $J_e^{0,7,9,19,22–28}$. The analysis of the frequency-dependent data ($|\eta^*(\omega)|$, $G'(\omega)$, $G''(\omega)$, ...) is much less developed due to its inherent complexity. It is generally accepted, however, that the introduction of

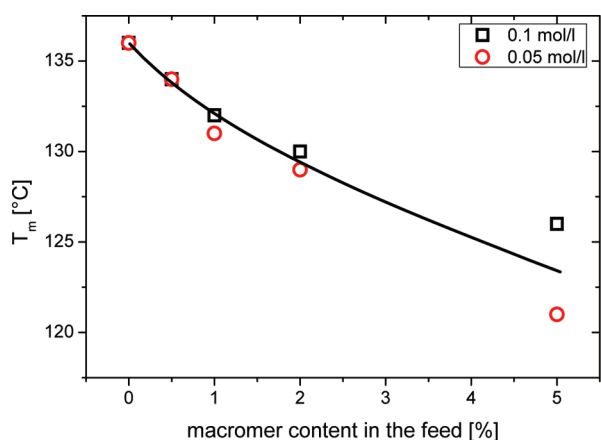


Figure 2. Dependence of the melting point of LCB-PE at high (0.1 mol/L) and low (0.05 mol/L) ethylene concentration on the content of macromer in the feed.

long-chain branches leads to the appearance of additional relaxation processes.^{7,8,29,30}

The analysis of the thermorheological behavior has been used for the characterization of a wide range of branched polyethylenes, too. The introduction of branches in general leads to an increase of the activation energy. For short-chain branched PE (LLDPE) a linear dependence between the weight content of the side chains and the activation energy E_a was found recently,^{31,32} generalizing an earlier method by Vega et al.³³ for different comonomer types. For highly long-chain branched LDPE activation energies between 55 and 75 kJ/mol have been reported,^{34–38} while lower values were established for LCB-mPE, which additionally behave thermorheologically complex;^{35,39} i.e., master curves cannot be constructed.

In this paper, we present results on the synthesis and characterization of the novel class of graft copolymers obtained by the copolymerization of ethylene/propylene macromers and ethylene. The characterization was carried out by SEC-MALLS, NMR, and rheological measurements. The rheological characterization focuses on the linear viscoelastic regime, especially on modulus functions, the zero shear-rate viscosity, and the temperature dependence of rheological data.

EXPERIMENTAL SECTION

Synthesis. *Chemicals.* Ethylene (99.8%) was provided by Linde and purified by passage through columns of BASF R3-11 oxygen scavenger and 4 Å molecular sieves for the polymerization. Propylene (99.8%) was provided by Gerling, Holz & Co. and was purified by the same process. Nitrogen was purified by passage through columns containing activated molecular sieves and Q-5 oxygen scavenger.

Pentane, hexane, toluene, and benzene were purified by passage through columns of activated alumina and BASF R3-11 oxygen scavenger. The polar solvents THF and CH_2Cl_2 were also purified by passage through two columns of activated alumina. THF- d_8 was stored over Na/benzophenone ketyl. CDCl_3 and CH_2Cl_2 were stored over P_2O_5 .

Methylaluminoxane (MAO) was provided by Akzo Nobel and purified by condensation.

Synthesis of EP-Macromers. All polymerization reactions were performed in a 1 L glass reactor (Büchi). The 1 L reactor was heated up to 90 °C and flushed with argon several times. Dry and powdered MAO was introduced to the reactor. The reactor was loaded with 400 mL of toluene. The solution was then saturated with propylene and ethylene.

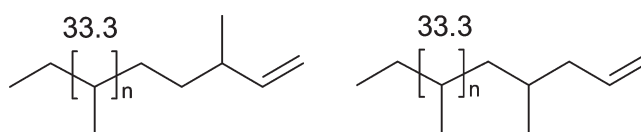


Figure 3. Signal correlated to the vinyl carbon atom in EP macromer. $\delta = 33.3$ ppm refers to the shift of the branching C in the macromer.

The ethylene pressure was kept stable by mass-flow control. The reaction was initiated by the injection of the desired volume of a stock solution of catalyst A into the reactor. The reaction was quenched after 2 h by the addition of 10 mL of ethanol. Then the reactor was emptied and washed with toluene and ethanol. 100 mL of dilute hydrochloric acid was added to the reaction solution, and the mixture was stirred overnight. The organic phase was separated and washed three times with water. It was concentrated under vacuum, and the waxy product was dried in the vacuum oven overnight at 40 °C.

Synthesis of Long-Chain Branched Polyethylene. The 1 L reactor was heated together with EP macromers at 60 °C for 1.5 h, and 400 mg of dry and powdered cocatalyst MAO was introduced to the reactor. The reactor was filled with 200 mL of dry toluene. Hydrogen gas was fed to the reactor for 2 min, and the solution was saturated with ethylene under stable pressure by mass-flow control. The reaction was initiated by injection of the desired volume of a solution of the fluorenyl catalyst ($[\text{Ph}_2\text{C}(2,7\text{-di-}t\text{-Bu}_2\text{Flu})(\text{Cp})]\text{ZrCl}_2$) into the reactor.

The copolymerization reaction was quenched after 2 h by the addition of 10 mL of ethanol. The reactor was emptied and washed with toluene and ethanol. 100 mL of dilute hydrochloric acid was given to the reaction solution, and the mixture was stirred overnight. The polymer solution was strained by suction filtration and washed three times with ethanol. The product was dried under vacuum in an oven overnight at 40 °C.

Purification of Long-Chain Branched Polyethylene. Soxhlet extraction was used to purify the long-chain branched polyethylene. The residual ethylene/propylene macromers of low molar mass were separated from the LCB-PE of high molar mass by making use of the property that, in contrast to the LCB-PE, the macromers are soluble in toluene. Toluene was put into a flask. The flask was heated, and the toluene gas rose up through the condenser. Then the condensed solvent dropped into the Soxhlet tube and perfused the product in the paper thimble. The hot toluene extracted ethylene/propylene macromers from the product. When the level of solvent was higher than the U-shaped side arm, the solvent with the dissolved low molar mass fraction was drained into the flask.

NMR. The macromer incorporation was determined by ^{13}C -labeled measurements at 100 °C (Bruker Avance 400 spectrometer). NMR samples were dissolved in hexachlorobutadiene referenced against 1,1,2,2-tetrachloroethane- d_2 .

Differential Scanning Calorimetry. The melting and glass transition temperatures of the polymers were measured by DSC. The measurements were carried out on a Mettler Toledo DSC 821. Indium with a melting point of 156.61 °C was used as a calibration standard. The sample for the measurements of about 5 mg was kept in aluminum pans. The heating rate was 20 °C/min, and the temperature ranged from –100 to 200 °C.

SEC-MALLS. The molecular characterization of the products were performed in 1,2,4-trichlorobenzene at 140 °C using a high-temperature SEC (Waters 150C) coupled with a multiangle light scattering instrument (Dawn EOS, Wyatt). Details of the experimental setup, the measuring procedure, and the evaluation of the data are given elsewhere.^{15,18}

Rheology. The rheological characterization was performed with a Bohlin/Malvern Gemini using an electrically heated nitrogen purged oven with a 25 mm parallel-plate geometry. Dynamic-mechanical tests were carried out at 150 °C as a standard and at 170, 190, 210, and 230 °C

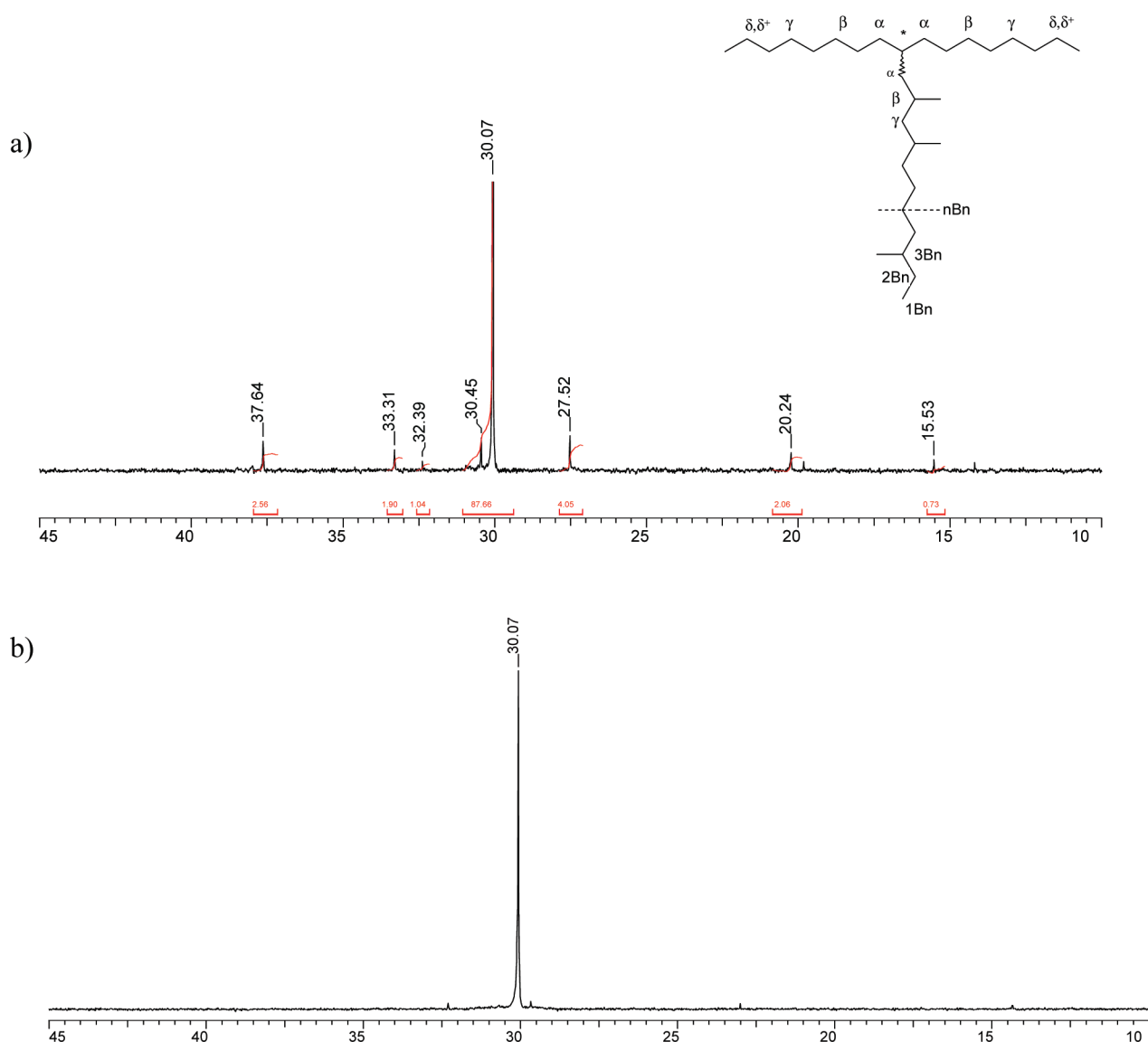


Figure 4. ^{13}C NMR spectra of MM-PE (a) and homo-PE (b) obtained by $[\text{Ph}_2\text{C}(2,7\text{-di-}t\text{-Bu}_2\text{Flu})(\text{Cp})]\text{ZrCl}_2/\text{MAO}$. The small peaks in MM-PE correspond to the carbons in the proximity of the methyl branches of the macromers.

to extend the frequency regime. Creep and creep recovery tests were performed at 150 °C in the linear range of deformations to determine η_0 . A more in-depth description of the testing methods used is given elsewhere.¹⁵ The thermal stability was proven by performing a frequency sweep at 150 °C as the first and the last test with each sample after preceding measurements. If the two tests agree within $\pm 5\%$ for all frequencies in both $G'(\omega)$ and $G''(\omega)$, it was concluded that the sample's thermal stability limit was not exceeded. In general, the materials were found to be very stable, which is in accordance with results on other samples obtained earlier using this catalyst.^{7,17,40}

For a further analysis, relaxation spectra were calculated according to the method of Stadler and Bailly.^{41,42}

RESULTS

Synthesis. LCB-PEs were synthesized in two steps. First, the EP macromers were generated, and then copolymerizations were run using the MAO activated fluorenyl catalyst $[\text{Ph}_2\text{C}(2,7\text{-di-}t\text{-Bu}_2\text{Flu})(\text{Cp})]\text{ZrCl}_2$, which has shown to

be a very successful catalyst for comonomer incorporations into LLDPEs.^{7,43}

Fluorenyl-based catalysts produce PEs with very high molar masses ($> 1 \times 10^6$ g/mol), which create problems for rheological measurements due to their very long relaxation times. The molar masses of the materials were regulated by the addition of hydrogen as explained later in this section.^{18,44}

EP-macromers with $M_w = 8000$ g/mol were used to generate LCB-PEs due to their higher solubility and the higher content of propylene in the chain compared to EP-macromers with a higher molar mass, which feature a lower propylene content.⁴ Polymerization was performed for 2 h, and the ethylene consumption was monitored by a mass flow control system. The bimodal copolymer fractions were purified by washing with hot toluene and Soxhlet extraction. This method resulted in the synthesis of LCB-PEs with novel properties by a controlled insertion of comonomers.

Table 1 shows the synthesis conditions along with the molecular data and the zero shear-rate viscosity of the macromer polyethylenes. MM stands for macromer followed by a number designating

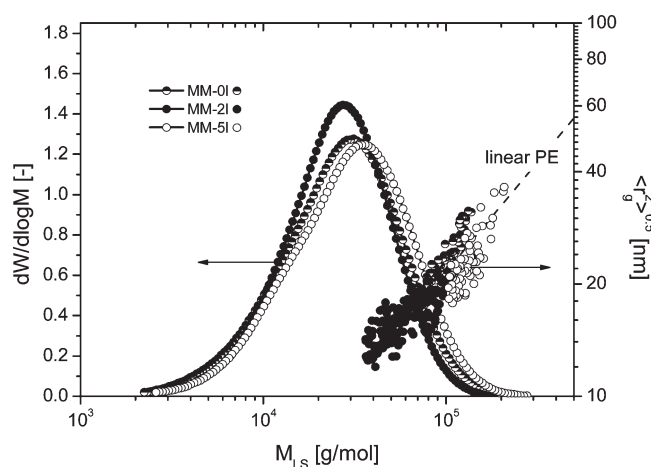


Figure 5. Molar mass distributions and radii of gyration for the samples prepared at low ethylene pressure (MM-0l: no macromer; MM-2l: 2% macromer; MM-5l: 5% macromer in the feed).

the molar content of macromer in the feed (0–5 mol %). The *h* and *l* indicate high and low monomer (ethylene) concentration, respectively, which, as the hydrogen content in the reactor was kept constant throughout the syntheses, varies the ratio of ethylene to hydrogen. This ratio determines the molar mass, as the likeliness of hydrogen leading to a termination of the sample depends on the concentration of hydrogen relative to that of the monomers.⁴⁵ As a consequence, the molar mass of the “*h*-samples” is adjusted to $M_w \approx 100$ kg/mol, while the “*l*-samples” have a molar mass of $M_w \approx 33$ kg/mol, only.^{4,18}

Differential Scanning Calorimetry. The melting point of the LCB-PEs was investigated by DSC. The comparison of melting points shows differences between the homopolyethylenes (MM-0l and MM-0h) and the long-chain branched samples. The melting point is reduced from 136 to 121 °C, even at a very low content of incorporated macro-monomers (Figure 2).

The melting temperatures T_m for different macromer contents n_c are not distinctly different from conventional LLDPE with various comonomer contents, despite the fact that the macromers are much longer.⁴⁶ This means that the melting point is distinctly higher than the values being expected from the weight content w_c .⁴⁷ The MM-PEs have a weight macromer content w_c of up to 60 wt % and still crystallize reasonably well. Furthermore, the single melting point is a clear indicator for the existence of copolymers and not blends, as a blend component would leave the melting point of the PE unchanged.

NMR. For a quantification of the branches, the materials synthesized in this work the inverse gated decoupled ^{13}C NMR was used. The carbon atom, at which the side chain was attached, could not be detected directly in the LCB-PEs by ^{13}C NMR measurements. This can be due to either an overlap of the carbon signal due to the coupling of the macromer with other signals or the very low effective concentration of the branching carbon atoms. The signal $\delta = 33.3$ ppm in the EP macromer was taken as a reference for the carbons carrying methyl groups (Figure 3). Thus, the methyl content of the total sample was determined, whose value is directly proportional to the macromer content, which is given in Table 1.

As the signals of the CH_2 moiety in both the LCB-PE and the EP macromer are around $\delta = 30$ ppm, the overlapping signal coming from the EP macromer was extracted from that of the main

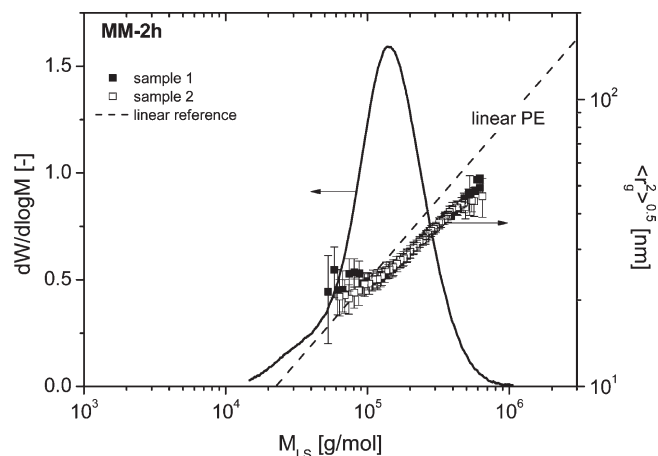


Figure 6. Molar mass distribution and radius of gyration of the sample MM-2h prepared at high ethylene concentration ($c = 0.1$ mol/L, 2% macromer in the feed). Two samples are shown to demonstrate the reproducibility of the experiment.

LCB-PE signal. The ^{13}C NMR spectrum of HDPE and LCB-PE are shown in Figure 4. The signals from the EP macromer are clearly observed as the extra peaks in the spectrum (Figure 4a) compared to that of the homopolyethylenes (Figure 4b).

SEC-MALLS. Broad molar mass distributions and long-chain branches can have a similar effect on some rheological properties of a material. In order to assess the effect of long-chain branching, the materials were measured by size exclusion chromatography coupled with multiangle laser light scattering (SEC-MALLS).⁴⁸

The multiangle light scattering (MALLS) detector measures the radius of gyration. The presence of long-chain branches leads to a decrease of the radius of gyration $\langle r_g^2 \rangle^{0.5}$, compared to the fraction of a linear material of the same molar mass.

The molar mass distribution (MMD) and $\langle r_g^2 \rangle^{0.5}$ are given in Figure 5 for materials prepared at low ethylene concentration (0.05 mol/L) and different macromer concentrations in the feed. From the MMD it is seen that the samples are unimodal, indicating that the purification step was successful in removing the not incorporated macromers. For the materials shown in Figure 5 $M_w/M_n \approx 2$ is found (see Table 1), which is typical of metallocene-based PE. Because of the quite low molar mass of the materials the scatter of $\langle r_g^2 \rangle^{0.5}$ is so high that it cannot be decided whether long-chain branches are present in the samples.

The materials prepared at higher ethylene concentration ($c = 0.1$ mol/L) and different macromer feeds were also analyzed by SEC-MALLS. As an example, the MMD of the material with 2% macromer in the feed is presented in Figure 6. It is unimodal, and therefore, the material does not contain any noticeable residual EP macromers. In contrast to the samples in Figure 5, a significant contraction of $\langle r_g^2 \rangle^{0.5}$ was found for this sample in comparison to the linear PE (Figure 6), indicating the existence of long-chain branches. This clear result is due to the fact that the molar masses and, thus, the resolution of the MALLS are higher.

GPC-MALLS measurements were also performed for the other materials prepared at higher ethylene pressures with varying macromer feeds. $\langle r_g^2 \rangle^{0.5}$ of all the materials deviates from the linear reference, and contractions are found for all the samples (Figure 7). These SEC-MALLS measurements indicate that the materials prepared with a feed of 1, 2, and 5% of macromer contain some long-chain branches.

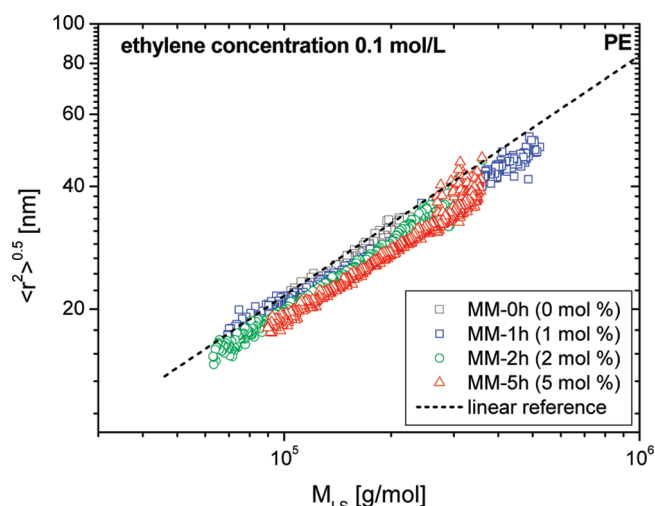


Figure 7. Radius of gyration as a function of the absolute molar mass M_{LS} of the samples prepared at high ethylene pressure and different amounts of macromer (0–5% macromer) in the feed.

The comparison between the data of the LCB-PEs shows that $\langle r^2 \rangle^{0.5}$ of the materials deviates the more strongly from the linear reference the higher the amount of macromer in the feed. This leads to the conclusion that the higher the macromer content in the feed, the higher the LCB content in the final polymer. Compared to normal LCB-PE, however, the deviation from the linear reference does not increase much with rising molar mass.^{18,49–51}

Using the data in Table 1, it is possible to get a more quantitative insight into the molecular structure of the comb PE. The macromer weight content w_c increases with growing feed. Following from n_c more than 10% of the available macromer is incorporated. As similar incorporation ratios are known for conventional comonomers (C8–C24) with this catalyst,^{7,43} the length of the comonomer/macromer does not seem to play a role for the insertion process. Because of the high molar mass of the macromer—several hundred times larger than conventional comonomers—very high weight contents are obtained as Figure 8a shows.

The backbone molar mass M_w^{bb} calculated according to

$$M_w^{bb} = M_w(1 - w_c) \quad (1)$$

is discussed in Figure 8b. The data indicate that the molar mass of the backbone decreases significantly upon incorporation of macromers. The trend of M_w^{bb} is identical for both ethylene concentrations, when normalized with the molar mass of the samples without macromer addition M_w^0 . The fact that the catalyst reacts very susceptible to hydrogen makes the correlation somewhat error afflicted.⁵²

Rheological Investigations. The zero shear-rate viscosities were determined from creep tests by plotting $t'/J(t')$ as a function of time in the linear range of deformation.^{53,54} t' is the creep time, and $J(t')$ is the creep compliance. Figure 9 shows that the plateau value and, therewith, the zero shear-rate viscosity η_0 is reached for MM-2h after about 6000 s. However, it is not possible to attain a plateau value for MM-1h within this time window; thus, it can only be concluded that the zero shear-rate viscosity η_0 of MM-1h is distinctly higher than 10^8 Pa·s.

Zero Shear-Rate Viscosities η_0 . The dependency of the zero shear-rate viscosity η_0 on the absolute molar mass M_w is a powerful relation to detect long-chain branches and to gain some qualitative

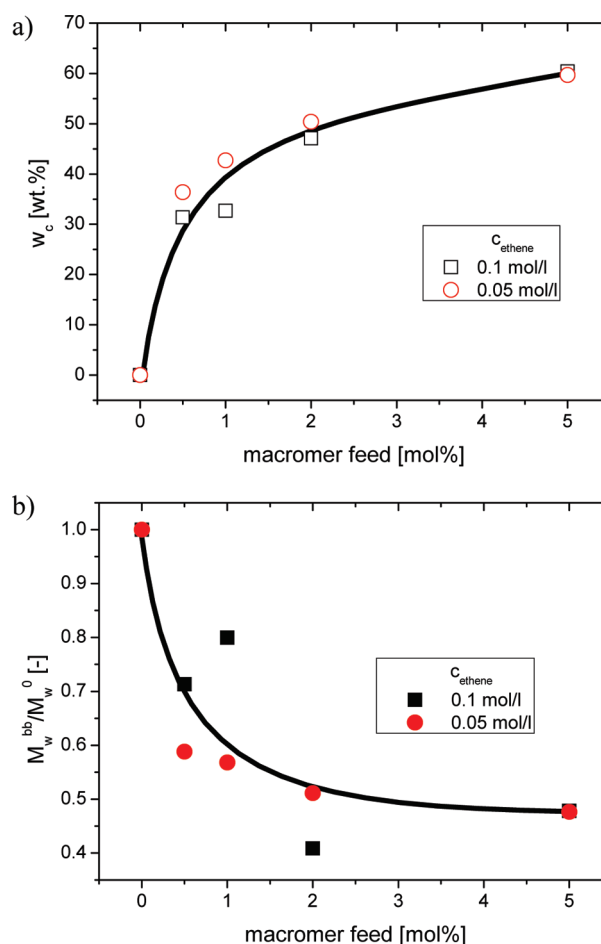


Figure 8. (a) Weight content of macromer (open symbols) and (b) reduction of backbone molar mass (filled symbols) in relation to the samples without macromer in the feed as a function of macromer feed. Lines drawn to guide the eye.

insight into the long-chain branching structure.^{24,55} In order to compare the new class of materials investigated in this paper to “normal” LCB-mPE, the results obtained in our previous papers are plotted in Figure 10 as the gray area, which encompasses the values available to the authors (about 60 materials).^{7,8,18,56} Although it was not possible to measure the zero shear-rate viscosity η_0 of any of the MM-PE samples with a molar mass M_w above 100 000 g/mol, it becomes immediately evident that the high molar mass samples distinctly deviate from the linear reference, while the low molecular samples are very close to the reference line of the linear products, which has been discussed in detail before.⁴ The high molar mass MM-PE differ more distinctly from the η_0 – M_w relation for linear polymers in comparison to the “normal” LCB-mPE; i.e., they have a higher zero shear rate viscosity increase factor η_0/η_0^{lin} than the “normal” LCB-mPE, if compared at the same M_w . In general, the actual zero shear rate viscosity η_0 is expected to become higher by at least a factor of 10 than the maximum viscosities plotted in Figure 10 for all samples with $M_w > 100$ 000 g/mol.

This strong deviation raises the question about the origin for this unusual behavior. The NMR spectroscopy showed a significant amount of methyl side groups in the samples, which can only stem from the macromers. However, as stated before, SEC-MALLS did not give any hint to unbound macromers, hence, it can be assumed that all of them are incorporated into the polymer

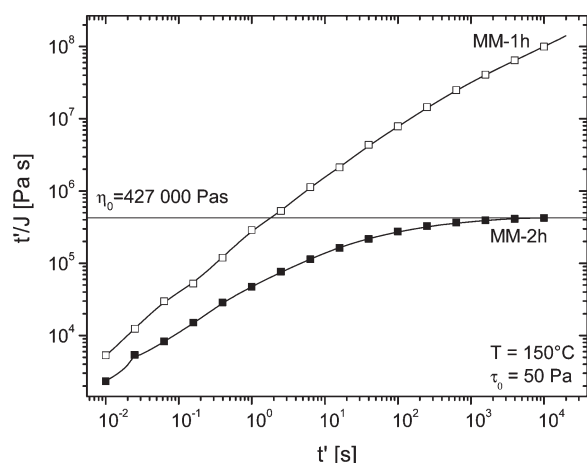


Figure 9. Creep time t' divided by creep compliance $J(t')$ as a function of creep time for MM-1h and MM-2h.

main chain. But the question remains how the branching topography looks like. From the probable reaction mechanism, it can be assumed that the structure is most likely comb-like and that the macromers are not part of the backbone.⁵⁷

Nevertheless, there is no way to conclude this from the molecular characterization directly. An alternative possibility would be a tree-like morphology. However, this can be ruled out by the η_0 – M_w plot, as tree-like morphologies, typical of LDPE and dendrimers, result in data below the η_0 – M_w relation for linear polymers.^{36,37,58} Values for combs, however, are found distinctly above the η_0 – M_w relation for linear polymers as long as the arms are not too short and too numerous.^{21,59,60} On the basis of the sample MM-0h, which according to $\eta_0(M_w)$ seems to be slightly long-chain branched itself, few combs with star-like backbones can be expected.

As it is justified to assume from the reaction mechanisms, SEC-MALLS, NMR characterization, and the rheological measurements as well that the dominating structure of the MM-PEs is the comb, the zero shear rate viscosities obtained can qualitatively be compared to the comb model for monodisperse polymers by Inkson et al.^{60,61} The highest viscosity found at certain molar mass M_w with the comb model is given in Figure 10 as the thick dashed line. It has to be considered, however, that the MM-PEs are polydisperse. Hence, only a qualitative comparison can be drawn.

Dynamic-Mechanical Experiments. The plot of the phase angle δ as a function of the magnitude of the complex modulus $|G^*|$ has been proven to be a valuable tool for the detection of long-chain branches for samples with a known MMD.^{18,19,62–64} A deviation of $\delta(|G^*|)$ for unknown samples from the curve of a reference established for linear samples of approximately the same MMD and M_w is a strong indicator for the presence of long-chain branching.

From Figure 11 it is obvious that even the homopolymer MM0 deviates distinctly from the linear reference, indicating a weak long-chain branching due to the characteristic phase angle δ_c ^{62,65} of 72°, which confirms the conclusions from the η_0 – M_w plot.¹⁸ The MM-PE samples show a very strong deviation from the linear reference. Fixing p_c is not possible for the MM-PE of the “h-series”, as the changes in slope are rather small. However, an approximate area for p_c can be given, which is indicated by the dashed ellipse in Figure 11. The positions of p_c , albeit not fixable exactly, are totally untypical of LCB-mPE in the molar mass range below $M_w = 300\,000$ g/mol. The shapes of the functions $\delta(|G^*|)$ of

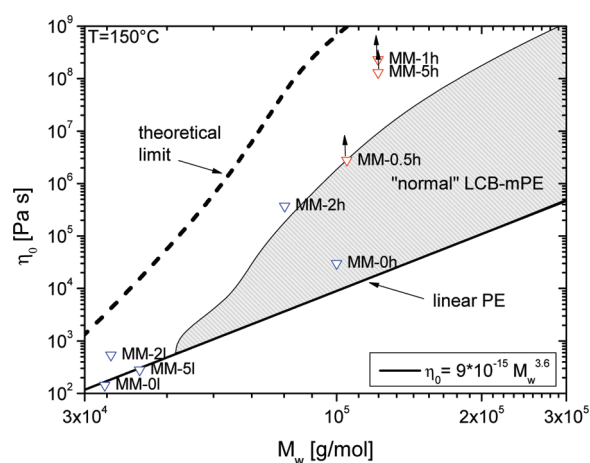


Figure 10. Correlation between the weight-average molar mass M_w and the zero shear rate viscosity η_0 . The gray area indicates the range, experimentally found for “normal” LCB-mPE.^{7,8,18}

the MM-PE have some similarities with a totally different class of materials—the highly branched low-density polyethylenes (cf. LDPE 1 and LDPE 2 in Figure 11), which are believed to have a tree-like branching structure and a very broad molar mass distribution.

The conclusion is that the MM-PE samples must possess long-chain branches with rather short relaxation times of the first hierarchical level. On the other hand, they also possess long terminal relaxation times (cf. Figure 9). Hence, it is concluded that two processes, a long and a short relaxation process, occur in case of the MM-PE. Such processes could be the relaxation process of short long-chain branches and the slow relaxation by fluctuation of the backbone. Short, entangled macromers attached to a backbone are a possible architecture for this type of behavior, as they are short enough to fluctuate quickly, thus showing short relaxation times. The fact that the terminal relaxation times are, nevertheless, very long is not a contradiction, as a backbone with long-chain branches attached to it cannot reptate, but relaxes by fluctuations, which are significantly slower than the reptation processes.^{60,67}

When comparing the shapes of the measured curves to the topography maps by Trinkle et al.⁶⁸ and the expanded version by Liu et al.,⁶⁹ to the data of the MM-PE, similarities appear. The topography map designates certain areas of the $\delta(|G^*|/G_N^0)$ plot to certain topographies.

According to Trinkle et al.,⁶⁸ the materials are located in the $\delta(|G^*|)$ plot (the critical point p_c with its coordinates δ_c and G_c) in the regime of stars and H-like polymers, close to the regime of highly entangled systems. However, Liu et al.⁶⁹ pointed out the topography map of Trinkle et al.⁶⁸ is incomplete, as too few model polymers were considered.

According to Liu et al.,⁶⁹ the MM-PEs' most likely topographies are either stars with an arm molar mass M_a around 25 kg/mol, an asymmetric star with M_a around 20 kg/mol, and one significantly longer arm, an H with a significantly longer backbone than the short arms (10 kg/mol) or a comb with few short arms (10 kg/mol). Although Liu et al.⁶⁹ used a molecular model⁶¹ and not experimental data, the advanced level of the molecular model nowadays allows for drawing a qualitative comparison. A stretched H and a comb with 2 arms can be considered to be almost identical structures.

The first possibilities—symmetric and asymmetric stars—are very unlikely because the synthesis conditions make the formation

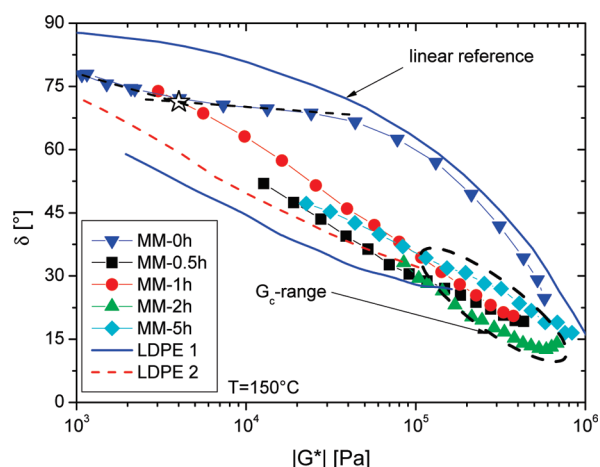


Figure 11. $\delta(|G^*|)$ plot of the reference polymer MM-0h without MM and of the samples with different MM-content. The linear reference was established elsewhere for linear mPE with $M_w/M_n \approx 2$.^{75,76} The critical point p_c of MM-0h is denoted by the ☆ symbol.

of stars with rather long arms rather unlikely. The “stretched H” and the “comb with few arms”, however, closely resemble what would be expected from the synthesis conditions for $M = M_w$. Even the length of the side chains ($M = 10$ kg/mol) is rather similar.

Although a clear assignment to a certain topography is not possible, the topography maps indicate that the conclusion from the reaction mechanism that the synthesis produces structures that can be designated as combs with few arms or stretched H and not other highly branched structures is plausible.

A similar structure from the point of view of hierarchical relaxation is found in low-density polyethylenes (LDPE), which are believed to have a tree-like morphology with chain segments in the same range as the macromers in the MM-PEs. The clear difference, however, lies in the fact that LDPE has a morphology with a branched backbone, comparable to a Cayley tree. Nevertheless, recent experiments on tree-like model polymers and their modeling have demonstrated that the differences in the rheological behavior between different topographies become the smaller the more complex the topography.^{58,70–74}

To illustrate this point, results on two typical LDPEs are also presented in Figure 11. LDPE 1 is a high molecular LDPE, previously studied in uni- and biaxial elongation,^{35,74} and LDPE 2 is a lower molecular grade.³⁵

Viscosity Functions. Figure 12 shows the viscosity functions $|\eta^*(\omega)|$ of the MM-PEs of the “h”-series. For comparison, also the viscosity function of LDPE 1 and the mLLDPE L4^{32,77,78} are plotted in the same figure. L4 has a molar mass very close to that of the MM-PEs of the “h”-series ($M_w = 114$ kg/mol), and it is proven to be strictly linear. The degree of short-chain branching is approximately equivalent to the comonomer content of the MM-PE (stemming from the methyl short-chain branches of the macromers).

MM-0h shows a small deviation in shape from the linear reference L4, which is typical of lightly branched LCB-mPE.^{76,79,80} However, this deviation is relatively small in comparison to the MM-PE, which differ from the linear reference by a factor of up to 1000 at $\omega = 0.01$ s^{−1}. The MM-PEs present a different type of viscosity function in comparison to regular LCB-mPE in the molar mass range between $M_w = 50$ and 200 kg/mol (e.g., MM-0h). The slope of

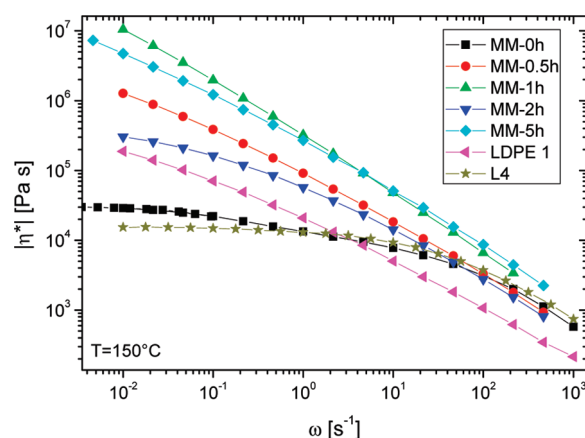


Figure 12. Viscosity functions $|\eta^*(\omega)|$ of the “h”-series MM-PEs in comparison to LDPE 1 and mLLDPE L4.

$|\eta^*(\omega)|$ decreases continuously with decreasing frequency (in double-log scaling); additionally, a slight leveling off at low frequencies can be observed. This behavior is untypical of LCB-mPE (here, two clearly separated main relaxation times would be expected, which lead to a more or less constant slope between them), but it is in close resemblance of the viscosity function of high molecular LDPEs such as LDPE 1, plotted also in Figure 12. However, the viscosity at high frequencies of the mPEs (L4, MM-0h, and all MM-PE samples) is about 3 times higher than for LDPE 1.

These differences indicate that the entanglement structure of the MM-PE samples is similar to the mPEs, despite their high level of long-chain branching. LDPE is lower in viscosity at high frequencies and, thus, seems to possess a looser entanglement network, which is caused by the fact that LDPEs have significant amounts of unentangled, low molecular components (which lead to M_n of LDPE typically below 30 kg/mol).^{36,81,82} Furthermore, it has to be considered that LDPE 1 has a molar mass M_w around 350 kg/mol, which is about 250% higher than the MM-PEs, although the latter have significantly higher viscosities in the whole range of frequencies, especially at low frequencies. This is a very good indicator that the MM-PEs are fundamentally different in their behavior from classical LDPEs, but also that they show clear differences at low frequencies as compared to the linear L4 or LCB-mPE MM-0h. Hence, they can be considered to be a different class of PE, with viscosity functions just between LDPE and LCB-mPE.

The Supporting Information contains graphs of the viscosity and modulus functions of the MM-PEs.

Thermorheological Behavior. From the thermorheological behavior conclusions can be drawn with respect to the branching structure of polyethylenes.^{31–35,39,40,58,78} It was investigated for the samples of the high molar mass series (“h”-series) with 0, 0.5, and 2 mol % macromer feed.

To find out whether a material is thermorheologically complex or simple, it was shown that it is straightforward to analyze the $\delta(|G^*|)$ plot.^{35,64,83–85} A temperature independency of $\delta(|G^*|)$ indicates a thermorheologically simple behavior. From Figure 13 the material MM-0.5h appears to be thermorheologically simple at a first glance, as the curves at different temperatures approximately fall together. Viewing the area marked by the dashed box more closely, however (see inset), it becomes evident that an increase of T results in a slight enhancement of $\delta(|G^*|)$. Although the effect is quite small (e.g., only 3.2° at 350 000 Pa), it points to a

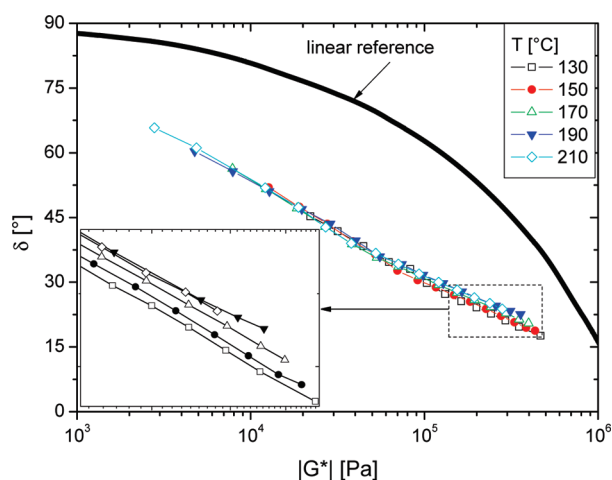


Figure 13. $\delta(|G^*|)$ plot of MM-0.5h at different T .

thermorheological complexity due to its systematic nature. This deviation, however, is small in comparison to LCB-mPE.³⁵

For the MM-PE samples with 2 mol % macromer feed, the effect related to thermorheological complexity is found to be even smaller. The reason for this behavior lies in the fact that the higher macromer content leads to a more “homogeneous” distribution of the macromer chains.

For MM-PE-2h, the macromer content is 50% higher than for MM-PE-0.5h, which supports the assumption of more molecules being similar than in the case of few macromers, only. It was concluded previously that one of the factors contributing to the amount of thermorheological complexity is the level of structural inhomogeneity in the sample, which is the reason why LDPE, which does not have significant amounts of high molar mass linear chains, shows a smaller thermorheological complexity than LCB-mPE, which typically consists of more than 30% linear chains.^{35,51,86}

MM-PE exhibits a thermorheological complexity, which is similar to that of LCB-mPE. However, due to the different shape of the $\delta(|G^*|)$ plot, the features of the thermorheological complexity appear different and become obvious at low δ , only. This behavior will be discussed in detail elsewhere along with other thermorheologically complex samples.⁸⁶ Nevertheless, the result is another hint to the existence of branching at least for the sample MM-0.5h.

CONCLUSIONS

The use of macromers for introducing long-chain branches into HDPE chains makes it possible that comb-like polymers (MM-PE) with a linear or star-like backbone are formed. From SEC-MALLS and NMR results, it can be concluded that the vast majority of the macromers occurring in the material after purification is chemically bonded to the HDPE backbones.

The rheological data measured support this conclusion. The values for the MM-PEs lie distinctly above the η_0 – M_w relation for linear PE and even above those of conventional LCB-mPEs. Taking the supposed degree of long-chain branching into account, which is significantly higher than for normal LCB-mPE, the classical highly branched low-density polyethylene (LDPE) with a tree-like topography could be expected to come close to the MM-PE. The important difference between the MM-PEs and LDPE, however, are their opposite positions with

respect to the reference line for linear PE in the η_0 – M_w plot. This finding alone is already a good indicator that the resulting branching architecture of the MM-PE synthesis is not tree-like but rather star-like or comb-like. As experiments on materials of such architectures and their theoretical descriptions have shown, only star-like, H/pompom-like, and comb-like architectures lead to an increase in η_0 , while a tree-like morphology induces a decrease, if compared to η_0 of a linear product at the same M_w .^{9,20,60,61,71–73} The comb model of Inkson et al.^{60,61} suggests that the increase of the zero shear rate viscosity η_0 for combs in comparison to linear chains and even star-like PE of the same molar mass is the consequence of a (relatively) quick relaxation of the side chains followed by a much slower relaxation of the main chain by fluctuation instead of the much faster reptation process linear chains exhibit.

The shapes of the rheological functions $\delta(|G^*|)$ and $|\eta^*(\omega)|$ of the “h-series” are significantly different from typical LCB-mPE, especially in the range of molar masses M_w around 100 kg/mol. This finding suggests a topography different from the LCB-mPE, which regarded as blends of linear and star-shaped molecules.^{7,68} However, the rheological functions of the MM-PEs measured are relatively similar to those of high molar mass LDPE, despite the much broader MMD and the different topography of the latter.^{36,82,87,88} This finding is supported by results from the literature that the modulus functions of monodisperse Cayley trees and combs are similar to some extent.^{9,61,71–73}

The comb model of Inkson et al.^{60,61} and their experimental data suggest a similarity in the shapes of the rheological functions between combs and the MM-PEs investigated in this paper. The nearly constant slope of $|\eta^*(\omega)|$ of the MM-PEs can be explained by the overlapping of the side chain and main chain relaxations, which are smeared out due to polydispersity.

The MM-PEs also exhibit a previously not reported thermorheological behavior. An only relatively small degree of thermorheological complexity is observed at low phase angles δ but not at high δ . This finding is different from that of classical LDPE, for which a constant modulus shift factor b_T can be used for eliminating the thermorheological complexity.⁸³ It also does not resemble the thermorheological complexity observed for LCB-mPE, showing deviations of $\delta(|G^*|)$ at high δ and not at low δ .

A comb-like architecture, which is in accordance with the NMR data and does not contradict the proposed reaction mechanism, is therefore very probable.

The results show that from rheological experiments above quantitative conclusions with respect to the molecular structure are difficult to be drawn, particularly in the case of branching. There are certain limitations as different branching architectures can result in comparable rheological properties or vice versa.

It is interesting to note that the SEC-MALLS data do not show very significant differences between the samples. This fact emphasizes once more the analytical power of rheological experiments with respect to investigations on the branching architecture of polymers.

SUMMARY

By using vinyl-terminated macromers, it is possible to synthesize polyethylenes with a tailored degree of long-chain branching and a comb-like topography. While these samples have some similarity with classical LDPEs in terms of rheological behavior and level of branching, their viscosity is significantly higher and their molar mass distribution is much narrower.

■ ASSOCIATED CONTENT

S Supporting Information. Graphs of the viscosity and modulus functions of the MM-PEs. This material is available free of charge via the Internet at <http://pubs.acs.org>.

■ AUTHOR INFORMATION

Corresponding Author

*E-mail fjstadler@jbnu.ac.kr, fax +82-63-270-2306.

Present Addresses

[†]Dow Europe GmbH, Bachtobelstrasse 3, CH-8810 Horgen.

■ ACKNOWLEDGMENT

The authors thank the German Research Foundation and the "Human Resource Development (project name: Advanced track for Si-based solar cell materials and devices, project number: 201040100660)" of the Korea Institute of Energy Technology Evaluation and Planning (KETEP) grant funded by the Korea government Ministry of Knowledge Economy for the financial support and Mrs. I. Herzer (University Erlangen) for the GPC-MALLS-measurements.

■ REFERENCES

- Soares, J. B. P.; Hamielec, A. E. *Macromol. Theory Simul.* **1996**, *5* (3), 547–572.
- Sperber, O.; Kaminsky, W. *Macromolecules* **2003**, *36* (24), 9014–9019.
- Rulhoff, S.; Kaminsky, W. *Macromol. Symp.* **2006**, *236*, 161–167.
- Arikan, B.; Stadler, F. J.; Kaschta, J.; Münstedt, H.; Kaminsky, W. *Macromol. Rapid Commun.* **2007**, *28* (14), 1472–1478.
- Stadler, F. J.; Arikan, B.; Kaschta, J.; Rulhoff, S.; Kaminsky, W.; Münstedt, H. *Macromol. Chem. Phys.* **2010**, *211*, 1472–1481.
- Kokko, E.; Pietikäinen, P.; Koivunen, J.; Seppälä, J. V. *J. Polym. Sci., Part A: Polym. Chem.* **2001**, *39* (21), 3805–3817.
- Stadler, F. J.; Piel, C.; Klimke, K.; Kaschta, J.; Parkinson, M.; Wilhelm, M.; Kaminsky, W.; Münstedt, H. *Macromolecules* **2006**, *39* (4), 1474–1482.
- Stadler, F. J.; Piel, C.; Kaminsky, W.; Münstedt, H. *Macromol. Symp.* **2006**, *236* (1), 209–218.
- Lohse, D. J.; Milner, S. T.; Fetters, L. J.; Xenidou, M.; Hadjichristidis, N.; Roovers, J.; Mendelson, R. A.; Garcia-Franco, C. A.; Lyon, M. K. *Macromolecules* **2002**, *35* (8), 3066–3075.
- Hyun, K.; Wilhelm, M. *Macromolecules* **2009**, *42* (1), 411–422.
- Hyun, K.; Wilhelm, M. *Kgk-Kautschuk Gummi Kunststoffe* **2010**, *63* (4), 123–129.
- Kirkwood, K. M.; Kapnistos, M.; Hadjichristidis, N.; Vlassopoulos, D.; Leal, G. In *The nonlinear rheology of entangled linear comb polymer solutions*, The Society of Rheology 79th Annual Meeting, Salt Lake City, Utah, 2007.
- Ferry, J. D. *Viscoelastic Properties of Polymers*; John Wiley and Sons: New York, 1980.
- Dealy, J.; Larson, R. G. *Structure and Rheology of Molten Polymers - From Structure to Flow Behavior and Back Again*; Hanser: Munich, 2006.
- Stadler, F. J.; Piel, C.; Kaschta, J.; Rulhoff, S.; Kaminsky, W.; Münstedt, H. *Rheol. Acta* **2006**, *45* (5), 755–764.
- Stadler, F. J.; Kaschta, J.; Münstedt, H. In *Viscous and Elastic Rheological Characterization of Ethene-/α-Olefin Copolymers*, 78th Annual Meeting of The Society of Rheology, Portland, 2006.
- Stadler, F. J.; Münstedt, H. *J. Rheol.* **2008**, *52* (3), 697–712.
- Piel, C.; Stadler, F. J.; Kaschta, J.; Rulhoff, S.; Münstedt, H.; Kaminsky, W. *Macromol. Chem. Phys.* **2006**, *207* (1), 26–38.
- Auhl, D.; Stange, J.; Münstedt, H.; Krause, B.; Voigt, D.; Lederer, A.; Lappan, U.; Lunkwitz, K. *Macromolecules* **2004**, *37* (25), 9465–9472.
- Kraus, G.; Gruver, J. T. *J. Polym. Sci., Part A: Gen. Pap.* **1965**, *3* (1), 105–122.
- Fujimoto, T.; Narukawa, H.; Nagasawa, M. *Macromolecules* **1970**, *3* (1), 57–64.
- Masuda, T.; Ohta, Y.; Onogi, S. *Macromolecules* **1971**, *4* (6), 763–8.
- Roovers, J.; Toporowski, P. M. *Macromolecules* **1987**, *20* (9), 2300–2306.
- Gabriel, C.; Münstedt, H. *Rheol. Acta* **2002**, *41* (3), 232–244.
- Gabriel, C.; Kokko, E.; Löfgren, B.; Seppälä, J.; Münstedt, H. *Polymer* **2002**, *43* (24), 6383–6390.
- Malmberg, A.; Gabriel, C.; Steffl, T.; Münstedt, H.; Löfgren, B. *Macromolecules* **2002**, *35*, 1038–1048.
- Gabriel, C. *Einfluss der molekularen Struktur auf das viskoelastische Verhalten von Polyethylenschmelzen*; Shaker-Verlag: Aachen, 2001; Vol. Ph.D.
- Patham, B.; Jayaraman, K. *J. Rheol.* **2005**, *49* (5), 989–999.
- Malmberg, A.; Kokko, E.; Lehmus, P.; Löfgren, B.; Seppälä, J. *Macromolecules* **1998**, *31* (24), 8448–8454.
- Wood-Adams, P. M.; Dealy, J. M.; deGroot, A. W.; Redwine, O. D. *Macromolecules* **2000**, *33* (20), 7489–7499.
- Stadler, F. J.; Gabriel, C.; Münstedt, H. *Macromol. Chem. Phys.* **2007**, *208* (22), 2449–2454.
- Kessner, U.; Münstedt, H.; Kaschta, J.; Stadler, F. J.; Le Duff, C. S.; Drooghaag, X. *Macromolecules* **2010**, *43* (17), 7341–7350.
- Vega, J. F.; Santamaria, A.; Munoz-Escalona, A.; Lafuente, P. *Macromolecules* **1998**, *31* (11), 3639–3647.
- Laun, H. M.; Münstedt, H. *Rheol. Acta* **1978**, *17*, 415–425.
- Stadler, F. J.; Kaschta, J.; Münstedt, H. *Macromolecules* **2008**, *41* (4), 1328–1333.
- Stadler, F. J.; Becker, F.; Kaschta, J.; Buback, M.; Münstedt, H. *Rheol. Acta* **2009**, *48* (5), 479–490.
- Agarwal, P. K.; Plazek, D. J. *J. Appl. Polym. Sci.* **1977**, *21* (12), 3251–3260.
- Plazek, D. J.; O'Rourke, V. M.; Choy, I. C. *Proc. IUPAC Macromol. Symp.*, 28th **1982**, 852.
- Wood-Adams, P. M.; Costeux, S. *Macromolecules* **2001**, *34* (18), 6281–6290.
- Stadler, F. J. *eXPRESS Polym. Lett.* **2011**, *5* (4), 327–341.
- Stadler, F. J.; Bailly, C. *Rheol. Acta* **2009**, *48* (1), 33–49.
- Stadler, F. J. *Rheol. Acta* **2010**, *49* (10), 1041–1057.
- Piel, C.; Starck, P.; Seppälä, J. V.; Kaminsky, W. *J. Polym. Sci., Part A: Polym. Chem.* **2006**, *44* (5), 1600–1612.
- Hoff, M.; Kaminsky, W. *Macromol. Chem. Phys.* **2004**, *205* (9), 1167–1173.
- Kaminsky, W.; Piel, C.; Scharlach, K. *Macromol. Symp.* **2005**, *226* (1), 25–34.
- Mandelkern, L. *The Crystalline State*, 2nd ed.; American Chemical Society: Washington, DC, 1993; Chapter 4.
- Mäder, D.; Heinemann, J.; Walter, P.; Müllhaupt, R. *Macromolecules* **2000**, *33*, 1254–1261.
- Wang, W. J.; Kharchenko, S.; Migler, K.; Zhu, S. P. *Polymer* **2004**, *45* (19), 6495–6505.
- Tackx, P.; Tackx, J. C. J. *Polymer* **1998**, *39* (14), 3109–3113.
- Sugimoto, M.; Suzuki, Y.; Hyun, K.; Ahn, K. H.; Ushioda, T.; Nishioka, A.; Taniguchi, T.; Koyama, K. *Rheol. Acta* **2006**, *46* (1), 33–44.
- Resch, J. A.; Stadler, F. J.; Kaschta, J.; Münstedt, H. *Macromolecules* **2009**, *42* (15), 5676–5683.
- We found previously that the catalyst used produces a molar mass of 1 200 000 g/mol, under the synthesis conditions of the samples without macromer, when it is not regulated with hydrogen.⁷ Hence, even a small difference in the ratio of ethylene and hydrogen has a significant effect on the molar mass.
- Gabriel, C.; Kaschta, J. *Rheol. Acta* **1998**, *37*, 358–364.
- Gabriel, C.; Kaschta, J.; Münstedt, H. *Rheol. Acta* **1998**, *37* (1), 7–20.

- (55) Berry, G. C.; Fox, T. G. *Adv. Polym. Sci.* **1968**, *5*, 261–357.
- (56) Janzen, J.; Colby, R. H. *J. Mol. Struct.* **1999**, 485–486, 569–584.
- (57) Because higher olefins tend to terminate a growing chain, also a small fraction of the macromers are likely to be incorporated as terminal chain. Hence, these macromers act as backbone extensions.
- (58) Laun, H. M. *Prog. Colloid Polym. Sci.* **1987**, *75*, 111–139.
- (59) Roovers, J. *Polymer* **1979**, *20* (7), 843–9.
- (60) Inkson, N. J.; Graham, R. S.; McLeish, T., C. B.; Groves, D. J.; Fernyhough, C. M. *Macromolecules* **2006**, *39* (12), 4217–4227.
- (61) Das, C.; Inkson, N. J.; Read, D. J.; Kelmanson, M. A.; McLeish, T. C. B. *J. Rheol.* **2006**, *50* (2), 207–235.
- (62) Trinkle, S.; Friedrich, C. *Rheol. Acta* **2001**, *40* (4), 322–328.
- (63) Walter, P.; Trinkle, S.; Müllhaupt, R. *Polymer* **2001**, *46*, 205–213.
- (64) van Gurp, M.; Palmen, J. *Rheol. Bull.* **1998**, *67* (1), 5–8.
- (65) Defined as the intercept between the tangents laid through turning points of the curve around the minimum or shoulder in $\delta(|G^*|)$.
- (66) Chen, X.; Stadler, F. J.; Münstedt, H.; Larson, R. G. *J. Rheol.* **2010**, *54* (2), 393–406.
- (67) Park, S. J.; Shanbhag, S.; Larson, R. G. *Rheol. Acta* **2005**, *44* (3), 319–330.
- (68) Trinkle, S.; Walter, P.; Friedrich, C. *Rheol. Acta* **2002**, *41* (1–2), 103–113.
- (69) Liu, J.; Yu, W.; Zhou, C. *J. Rheol.* **2011**, *55* (3), 545–570.
- (70) van Ruymbeke, E.; Kapnistos, M.; Vlassopoulos, D.; Huang, T. Z.; Knauss, D. M. *Macromolecules* **2007**, *40* (5), 1713–1719.
- (71) van Ruymbeke, E.; Orfanou, K.; Kapnistos, M.; Iatrou, H.; Pitsikalis, M.; Hadjichristidis, N.; Lohse, D. J.; Vlassopoulos, D. *Macromolecules* **2007**, *40* (16), 5941–5952.
- (72) Kapnistos, M.; Vlassopoulos, D.; Roovers, J.; Leal, L. G. *Macromolecules* **2005**, *38* (18), 7852–7862.
- (73) Kapnistos, M.; Koutalas, G.; Hadjichristidis, N.; Roovers, J.; Lohse, D. J.; Vlassopoulos, D. *Rheol. Acta* **2006**, *46* (2), 273–286.
- (74) Stadler, F. J.; Nishioka, A.; Stange, J.; Koyama, K.; Münstedt, H. *Rheol. Acta* **2007**, *46* (7), 1003–1012.
- (75) Stadler, F. J. *Molecular Structure and Rheological Properties of Linear and Long-Chain Branched Ethene- α -Olefin Copolymers*; Sierke-Verlag: Göttingen, 2007.
- (76) Stadler, F. J.; Münstedt, H. *Macromol. Mater. Eng.* **2009**, *294* (1), 25–34.
- (77) Stadler, F. J.; Kaschta, J.; Münstedt, H. *Polymer* **2005**, *46* (23), 10311–10320.
- (78) Resch, J. A.; Stadler, F. J.; Kaschta, J.; Münstedt, H. *Macromolecules* **2009**, *42* (15), 5676–5683.
- (79) Stadler, F. J.; Münstedt, H. *J. Non-Newtonian Fluid Mech.* **2008**, *151*, 129–135.
- (80) Stadler, F. J.; Münstedt, H. *J. Non-Newtonian Fluid Mech.* **2008**, *151*, 227.
- (81) Otte, T.; Stadler, F. J.; Brüll, R.; Macko, T. *J. Chromatogr.* **2011**, 10.1016/j.chroma.2010.12.072.
- (82) Shirayama, K.; Okada, T.; Kita, S. *J. Polym. Sci., Part A: Polym. Chem.* **1965**, *3*, 907–916.
- (83) Kessner, U.; Kaschta, J.; Münstedt, H. *J. Rheol.* **2009**, *53* (4), 1001–1016.
- (84) Kessner, U.; Münstedt, H. *Polymer* **2009**, *51*, 507–513.
- (85) Stadler, F. J. *J. Rheol.* **2011** submitted.
- (86) Stadler, F. J.; Mahmoudi, T. *Rheol. Acta* **2011**, submitted.
- (87) Otocka, E. P.; Roe, R. J.; Hellman, M. Y.; Muglia, P. M. *Polymer* **1971**, *4* (4), 507–512.
- (88) Münstedt, H. *Rheol. Acta* **1979**, *18*, 492–504.